Anionically Stabilized Cellulose Nanofibrils via Succinylation Pre-Treatment in Urea-LiCl Deep Eutectic Solvent

Tuula Selkälä,[a] Juho Antti Sirviö,[a] Gabriela S. Lorite,[b] and Henrikki Liimatainen*[a]

Abstract: Deep eutectic solvents (DESs) are green chemicals that have the potential to be substituted for traditional solvents in chemical reactions. In this study, urea-LiCl DES was successfully used as a reaction medium in the anionic functionalization of wood cellulose with succinic anhydride. The effects of reaction temperature and time on the carboxyl content and yield were evaluated. The degree of polymerization and crystallinity analyses revealed that the DES was a non-degrading and non-dissolving reaction media. Three samples having the highest carboxyl contents were further nanofibrillated using a microfluidizer to a diameter of 2-7 nm observed via atomic force microscopy. Samples treated at 70-80 °C for 2 h gave the best outcome, resulting in highly viscose and transparent gel. The sample treated at 90 °C contained bigger nanoparticles and larger aggregates due to the occurrence of possible side reactions but resulted in better thermal stability than the two other samples.

Introduction

Organic solvents are an essential part of chemistry and materials science. They are used as raw materials in products (e.g. paints), in reactions, for instrument cleaning and as reaction media.[1] The majority of organic solvents are produced from oil. Many common volatile organic compounds (VOCs) used as solvents are flammable, non-biodegradable, toxic and harmful to the atmosphere due to their inherent properties.[1] The best option from an environmental point of view would be to avoid the use of solvents altogether or switch to more sustainable alternatives.[2,3]

Interest in the development of green chemistry alternatives to traditional organic solvents has grown recently. Examples of studied green solvents are fluorinated solvents,[4] supercritical fluids (e.g. CO_2),[5] biomass-derived solvents (e.g. glycerol)[6] and ionic liquids (ILs).[7–9] Even water at supercritical and/or subcritical state (pressurized hot water) can be considered as an alternative solvent for the extraction of polar and non-polar compounds.[10,11] Currently there is an immense interest in deep eutectic solvents (DESs).[12–17] DESs are mixtures of two or more acidic and alkaline components that can form synergetic effect with each other and act as solvents, reactants or even catalysts. They can be often prepared from green and bulk chemicals by applying a straightforward heating and mixing procedure. Moreover, many DESs are biodegradable[18,19] and have low vapor pressure[1] and relatively low toxicity[20,21]—all aspects that fit in the 12 Principles of Green Chemistry.[22]

In addition to the development of safer and sustainable solvents, there is a need for replacing oil-based products with biobased ones in uses such as packaging[23] and water treatment.[24–26] Cellulose is the most abundant natural polymer on Earth, and being non-food, it is an appealing raw material for biobased products. Cellulose is a renewable, biodegradable and nontoxic material that can be obtained, for example, from wood, plants and agricultural residues. Native cellulose has low inherent activity, but its properties can be tuned since it has three reactive hydroxyl groups per repeating unit, which enables the introduction of new functional groups and results in the production of new semi-synthetic materials. In addition, nanocelluloses, i.e. particles with at least one dimension in nanoscale (1-100 nm), open totally new areas for the utilization of biomass in high added value applications. Cellulose nanofibrils[27] are typically composed of elementary fibrils of cellulose fiber cell wall and their bundles, and they have a diameter of ca. 5-50 nm and a length of up to several micrometers. Nanofibrils can be liberated from cellulose solely by mechanical disintegration such as refining, grinding and homogenization (by homogenizers and microfluidizers). The high energy consumption of mechanical disintegration can be reduced by enzymatic, chemical[28–31] and/or solvent-assisted[32] pretreatments, which make the cellulose structure more prone to disintegration.

The introduction of negatively charged groups like carboxyl on cellulose fibers enhances their disintegration down to nano-scale due to electrostatic repulsion and structure swelling. For this purpose, ester-acid functionalities can be attached via esterification reaction between cellulose hydroxyls and cyclic anhydrides, like succinic anhydride (succinylation). Plenty of research has been done on the succinylation of cellulose in pyridine[33–36] and in ILs,[37–42] both with or without a catalyst. Solvent-free succinylation of wood cellulose has also been conducted.[43] Regarding nanocellulose production, mechanochemical succinylation in DMSO[44] has been previously reported. Succinylation of mercerized nanocellulose in pyridine has also been studied.[45] Activities on the use of DESs in cellulose functionalization have been minor so far, and they could offer a promising green media for succinylation reactions. However, the succinylation of cellulose in DES as a pretreatment for nanofibril production has not been reported before.

In this work we investigated succinylation of wood cellulose in DES made of cheap and safe raw materials and further

[a] T. Selkälä, Dr. J. A. Sirviö, Assoc. Prof. H. Liimatainen
Fibre and Particle Engineering Research Unit
University of Oulu
P.O. Box 4300, FI-90014, Finland
E-mail: henrikki.liimatainen@oulu.fi
[b] Dr. G. S. Lorite
Microelectronics Research Unit
University of Oulu
P.O. Box 4500, FI-90014, Finland

disintegration of functionalized cellulose into nanofibrils. A DES system comprised of urea and LiCl was selected as a reaction media for heterogeneous succinylation of softwood dissolving pulp, and nanofibrils were obtained using a microfluidizer after removal of DES. The succinylated celluloses were analyzed using diffuse reflectance infrared Fourier transform (DRIFT) spectroscopy and wide-angle X-ray diffraction (WAXD). The number of acidic groups were measured using a conductometric titration method, and the elemental composition was determined using a CHNS/O elemental analyzer. The degree of polymerization (DP) of the cellulose was determined using the limiting viscosity method. The obtained nanofibrils were comprehensively analyzed using WAXD, atomic force microscopy (AFM), viscosity measurements, optical transmittance measurements and thermogravimetric analysis (TGA).

Results and Discussion

Succinylation of cellulose in urea-LiCl DES

Anionic cellulose nanofibrils were produced through succinylation pretreatment of commercial dissolving wood cellulose pulp in urea-LiCl DES followed by nanofibrillation using a microfluidizer. Carboxyl groups were successfully introduced onto cellulose through ring-opening esterification reaction of succinic anhydride with cellulose hydroxyl groups in DES media, as shown in Scheme 1. No added catalysts, water or organic solvents were needed to carry out the reaction.

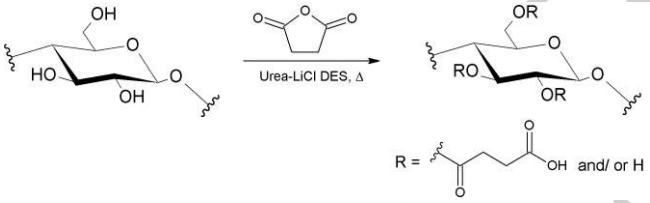

Scheme 1. Succinylation of cellulose in urea-LiCl DES.

The DES used as a novel succinylation reaction media was prepared by pre-mixing urea and LiCl (molar ratio of 5:1) followed by simultaneous heating and mixing until a clear, colorless liquid was formed (Figure 1A). According to our observations, the most crucial factor affecting the time needed for the DES formation was the mixing efficiency. In the beginning of the heating process the mixture wetted, densified and finally liquefied before turning clear. The addition of succinic anhydride and cellulose pulp (molar ratio of 10:1) to DES resulted in a homogeneous suspension in which the cellulose was evenly distributed in the form of solid fibers. As the reaction proceeded, the mixture became more transparent, gel-like and uniform in texture, indicating the efficient modification and swelling of the pulp fibers. The addition of ethanol stopped the reaction as it reacted with the remaining anhydride. The fibers separated from the reaction mixture in the form of slightly gel-like material, which had a higher water retention capacity than the original pulp, which indicated successful functionalization of the fibers since carboxyl groups are more hydrophilic than hydroxyl groups.[43] After washing the modified fibers with water, no visible differences with the original pulp and succinylated pulp were observed.

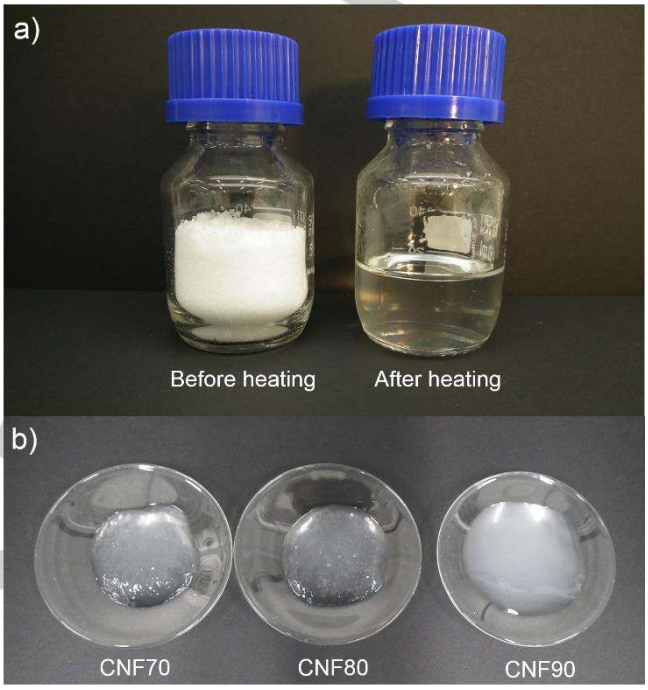

Figure 1. a) Images of urea-LiCl (molar ratio of 5:1) DES before heating and after making a homogeneous solution by heating at 80 °C, b) images of succinylated nanofibrils CNF70, 80 and 90 (0.5 % cellulose consistency).

The effect of different reaction temperatures and reaction times on the yields and carboxyl contents of the succinylated fibers are presented in Table 1. The yield decreased as the reaction temperature was increased up to 90 °C but started to increase as temperature was raised even further, up to 110 °C. In most cases the yield decreased as a function of reaction time, except with samples that reacted at 90 °C, in which the opposite effect was observed. In theory, the yield should be over 100 % because the reaction adds functional groups to the cellulose structure, increasing its weight. In practice, cellulose and residual hemicelluloses of the pulp can dissolve[46] during chemical treatment, which decreases the yield of the reaction. As the temperature was raised above 90 °C, the yield loss caused by the dissolution was compensated by the introduced functionalized groups. In addition to the conditions reported in Table 1, a reaction temperature of 60 °C was tested, but succinic anhydride did not dissolve in DES at that temperature.

The carboxyl content of the succinylated fibers followed an opposite temperature trend compared to the yield. The amount of carboxyl groups increased up to 90 °C, after which it started to decrease. Considering the reaction time, 2 h was sufficient to

achieve similar or even higher carboxyl content than with longer reaction times. In the temperatures between 80-110 °C, the reaction time of 24 h resulted in the lowest carboxyl contents. A plausible explanation for the results is that the temperature promoted the reactivity of cellulose, but at higher temperatures (above 90 °C) the cross-linking reaction[47] between the carboxyl groups and vacant hydroxyl groups in cellulose chains started to compete with the functionalization reaction, which reduced the amount of free carboxyl groups. Similar results have been reported before regarding the time and temperature dependence of succinylation reaction.[38,40,42]

Table 1. Reaction conditions, yields and carboxyl contents of succinylated cellulose samples.

Reaction temperature [°C]	Reaction time [h]	Yield after reaction [%]	Carboxyl content [mmol g^{-1}]
70	2	113.5	0.57
	6	112.4	0.35
	24	91.2	0.40
80	2	103.4	0.69
	6	101.0	0.71
	24	102.4	0.56
90	2	80.0	0.94
	6	82.3	0.95
	24	88.3	0.84
100	2	100.5	0.51
	6	98.5	0.62
	24	90.3	0.47
110	2	120.4	0.37
	6	104.1	0.39
	24	92.3	0.34

Nanofibrillation of succinylated fibers

The pulps modified at 70 °C, 80 °C and 90 °C for 2 h (samples SC70, SC80 and SC90) were selected for nanofibrillation due to their relatively high carboxyl contents. All samples were successfully individualized to cellulose nanofibrils and were named CNF70, CNF80 and CNF90. The fibers modified at 70 °C and 80 °C formed a thick, homogenous, transparent and gel-like material after three passes through the microfluidizer (Figure 1B, CNF70 and CNF80). The pulp modified at 90 °C, however, required prolonged homogenization treatment to form a turbid and fluid material (Figure 1B, CNF90).

Characteristics of succinylated fibers and nanofibrils

Figure 2 shows the DRIFT spectra of an unmodified dissolving pulp and succinylated samples SC70, SC80 and SC90. The bands appearing at around 3400 cm^{-1}, 2900 cm^{-1}, 1430 cm^{-1}, 1371 cm^{-1} and 899 cm^{-1} are associated with native cellulose.[48] The absorption at 3400 cm^{-1} is due to the OH stretching, and the one at 2900 cm^{-1} is due to the CH stretching. The band at 1633 cm^{-1} (spectrum a) corresponds to the OH bending mode of the absorbed water. The absorbance at 1430 cm^{-1} is associated with the HCH and OCH in-plane bending vibrations, while the band at 1371 cm^{-1} corresponds to the CH deformation vibration. Finally, the band at 899 cm^{-1} is attributed to the COC, CCO and CCH deformation modes and stretching vibrations. Compared to the dissolving pulp, the samples SC70, SC80 and SC90 exhibited a distinctive band at 1730 cm^{-1} assigned to the C=O stretching in carboxylic acids and esters, which confirmed the occurrence of esterification reaction between cellulose hydroxyl groups and succinic anhydride in DES.[33] The band is actually an outcome of two overlapping bonds—the absorption of carbonyl bonds in esters (1740 cm^{-1}) and in carboxylic acids (1700 cm^{-1}). Interestingly, only the sample SC90 exhibited an additional band at 1574 cm^{-1}, which corresponds to antisymmetric stretching of carboxylate anions.[47] The absence of bands at 1850 cm^{-1} and 1780 cm^{-1} confirmed that the modified pulps were free from unreacted succinic anhydride.[49]

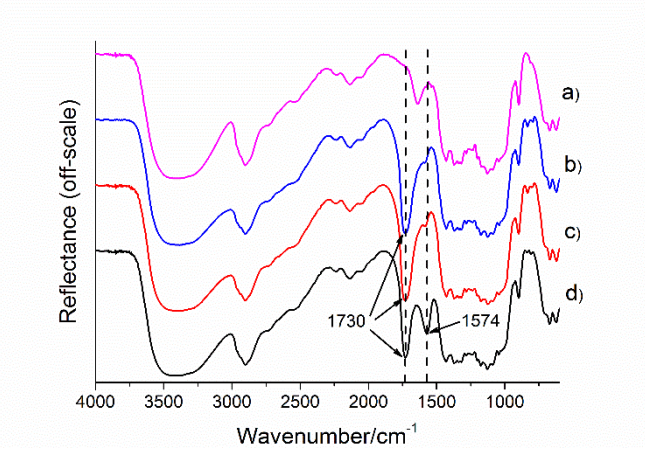

Figure 2. DRIFT spectra of a) dissolving pulp and succinylated celluloses b) SC70, c) SC80 and d) SC90. Absorption band at 1730 cm^{-1} is assigned to carbonyl stretching in carboxylic acids and esters and 1574 cm^{-1} to stretching of carboxylate anions.

The presence of carboxylate anions in the sample SC90 was further confirmed by measuring the pH of the samples. The pH of the samples SC70, SC80 and SC90 were 3.6, 3.7 and 7.0, respectively. The drastic change in pH may be caused by ammonia, which is a decomposition product of urea[50] and also a by-product in the carbamation of cellulose at high temperatures.[51] The carbamate group resulting from the reaction between cellulose and urea would have a characteristic band at

around 1713 cm^{-1},[51,52] but in this case it overlaps with the strong carbonyl bond absorptions discussed earlier and is thus undetectable. The formation of carbamate and/or ammonia in the reaction was studied by elemental analysis. In order to see if the nitrogen was bound to the cellulose structure as carbamate or if it was mainly present as a counter ion (NH_4^+), the sample was analyzed before and after an acid wash treatment, and the amount of nitrogen in the samples were compared (Table 2). The only sample containing a detectable amount of nitrogen before the acid wash was, as expected, the sample SC90, in which the amount of nitrogen decreased from 0.4 % to 0.1 %. Consequently, based on the DRIFT and the elemental analysis results, the nitrogen in the sample SC90 is present mainly in the form of ammonium ions and not as carbamate.

Table 2. Percentage of carbon, hydrogen and nitrogen in the dissolving pulp and succinylated fibers (SC70, 80 and 90) before and after acid wash.

Sample		C [%]	H [%]	N [%][a]
Dissolving pulp	before	42.8	6.6	0.2
	after	43.3	7.0	0
SC70	before	43.7	6.8	0
	after	43.5	7.0	0
SC80	before	43.5	5.5	0.1
	after	43.5	6.7	0
SC90	before	43.7	6.6	0.4
	after	43.1	5.1	0.1

[a] The detection limit of the analyzer was 0.2 %

The change in the length of the cellulose polymer chains was studied by measuring the degree of polymerization (DP). The decrease in the DPs of the succinylated samples was less than 10 % compared to the original dissolving pulp (Figure 3). Thus, it is likely that the succinylation done in urea-LiCl DES affects mainly the hydroxyl groups in the cellulose backbone, leaving the glycosidic bonds intact. The difference in the DPs of the samples SC70, SC80 and SC90 was negligible.

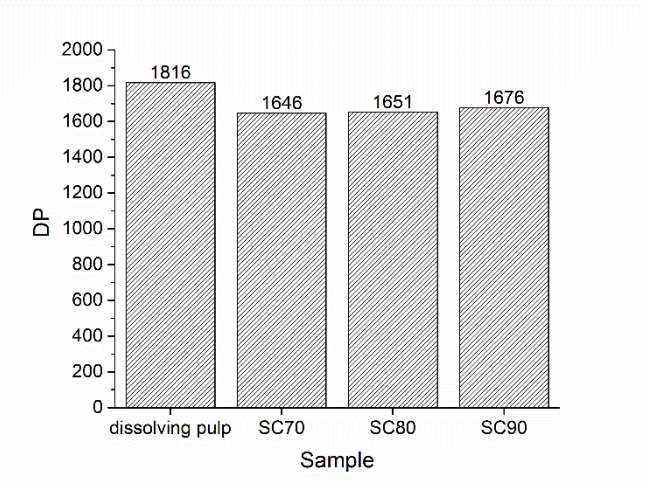

Figure 3. DPs of the dissolving pulp and succinylated fibers (SC70, 80 and 90).

The effect of succinylation and consequent mechanical treatment on the cellulose crystal structure was studied using WAXD (Figure 4). All X-ray diffractograms exhibited typical cellulose I peaks with the main 2θ diffraction angles around 18.5° and 26° (Co Kα radiation source), which indicated that the crystalline structure of the cellulose remained intact during the modification in DES and consequent mechanical nanofibrillation. Interestingly, the calculated crystalline indexes (CrI) of succinylated samples were slightly higher than the CrI of the pristine dissolving pulp (65.4 %). The CrI were 68.4 %, 69.0 % and 69.8 % for samples SC70, SC80 and SC90, respectively. The higher value is likely the result of the modification in DES, which dissolves parts of the remaining hemicellulose in the pulp.[46] Moreover, the CrI increased as the temperature was increased, which suggests that the dissolution is more pronounced in higher temperatures.

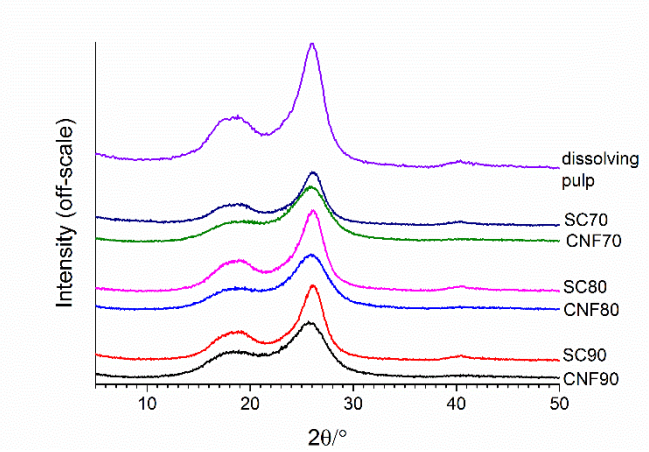

Figure 4. Diffractograms of dissolving pulp and succinylated fibers before (SC70, 80 and 90) and after nanofibrillation (CNF70, 80 and 90).

After mechanical nanofibrillation, the crystallinity of the samples decreased, resulting in CrI of 58.3 %, 57.4 % and 51.5 % for samples CNF70, CNF80 and CNF90, respectively (Figure 4). This decrease is assumed to be due to high shear forces that loosen the crystalline structure and cause the peeling of the cellulose chains on the crystallites.[53] As expected, the number of passes through the microfluidizer correlated with the decrease in the crystallinity. The sample exposed to highest number of passes through the microfluidizer (CNF90) experienced the highest decrease (18 %) in the crystallinity. The samples CNF70 and CNF80 were both passed through the microfluidizer only three times and had similar ~10 % decreases in the crystallinity.

Succinylated nanofibrils' morphology was characterized via AFM topography images. The images clearly showed that the samples had a network structure consisting of a mixture of nanofibril bundles and individual nanofibrils (Figure 5). In addition, the height profile of individual nanofibrils was evaluated (Figure 6). CNF70, CNF80 and CNF90 presented different height distribution ranges (0.5-4 nm, 1.5-4.5 nm and 1.5-7.5 nm, respectively). In addition, the height distribution of sample CNF70 was well-centered in 2.6±0.7 nm (Figure 6A), while CNF80 presented high proportion between 1.5-3 nm (Figure 6B). CNF90 showed not only a larger height distribution, but the sample also possessed a bimodal distribution centered at 3.1±0.8 nm and 4.6±0.8 nm (Figure 6C). These results suggest that the reaction temperature affected the succinylated nanofibrils' dimensions.

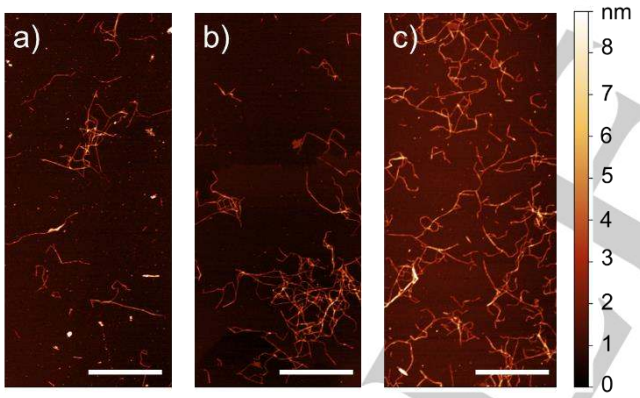

Figure 5. Representative AFM topography image for cellulose nanofibrils a) CNF70, b) CNF80 and c) CNF90. Scale bar: 1 µm.

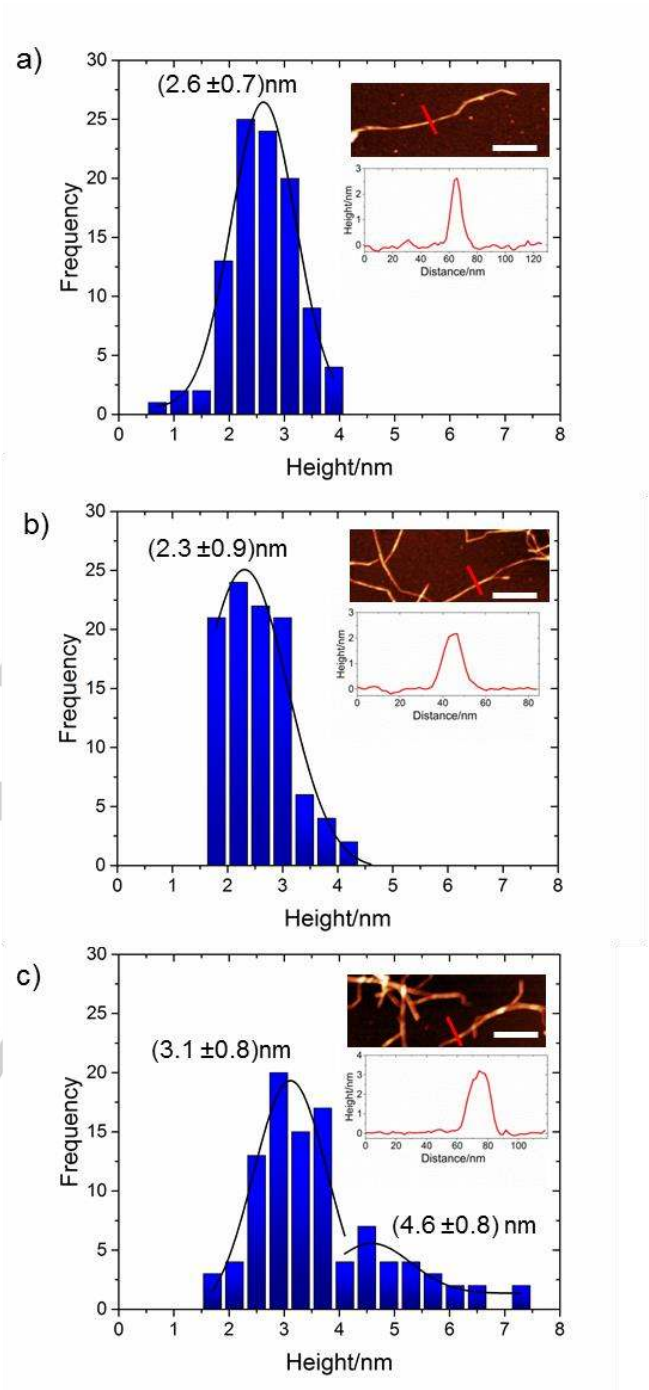

Figure 6. Height distribution for cellulose nanofibrils a) CNF70, b) CNF80 and c) CNF90. Gaussian fitting was used to evaluate the peak center as shown in each distribution. Inset: representative AFM topography image and correspondent height profile, scale bar: 200 nm.

The rotational viscosities of 0.2 % nanofibril suspensions of CNF70, CNF80 and CNF90 are presented in Figure 7. All samples expressed high viscosities and typical shear thinning properties, which is in line with previously reported results for anionic nanocelluloses.[28] However, contrary to previous findings, the viscosities decreased steadily as a function of increasing carboxyl content. The viscosity values at certain rotational speed decreased by ~50 % when changing the sample from CNF70 to CNF80, and the same trend was observed between CNF80 and CNF90. It is possible that the increased charge density from one sample to another reduced the hydrogen bonding necessary for the formation of a strong network of nanofibrils, thus lowering the viscosity.[53] Also the observed changes in the nanofibrils' dimensions between the samples may have influenced the viscosities. It should be noted that the viscosities were measured in low cellulose consistency due to the very high viscosities of the samples and that the carboxyl groups were in anionic form in all samples due to the pH adjustment performed before nanofibrillation.

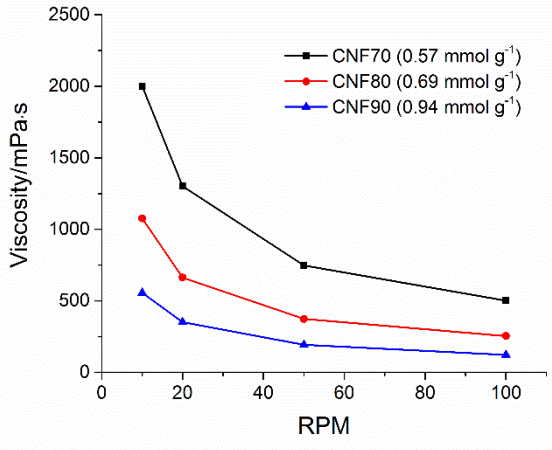

Figure 7. Viscosity of the 0.2 % cellulose nanofibril suspensions (CNF70, 80 and 90). The values in brackets refer to the carboxyl contents of the samples.

Optical transmittances (Figure 8) of dilute nanofibril suspensions (0.1 % cellulose consistency) of samples CNF70 and CNF80 were high (>75 %) at wavelengths of 350-800 nm, which indicated successful disintegration of succinylated celluloses to individual nanosized cellulose.[54] The results are consistent with our previous studies with anionic nanocelluloses obtained from oxidative pretreatments.[28] Sample CNF90 had lower optical transmittance as expected based on the visual inspection (Figure 1B) and AFM height profile (Figure 6), which indicated that the fibers were only partly disintegrated and contained some residual larger aggregates.

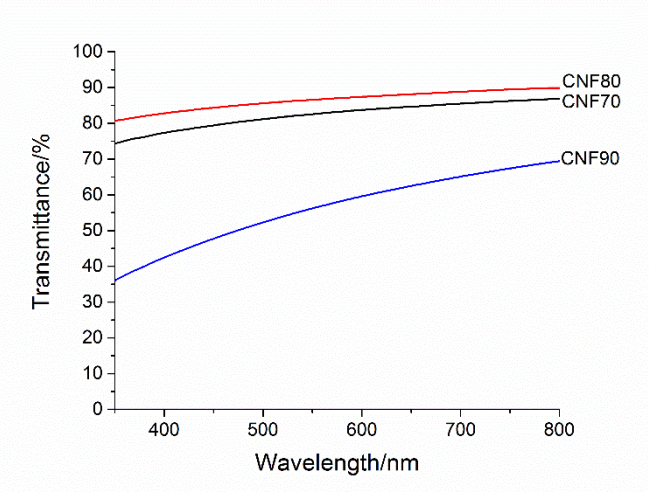

Figure 8. Optical transmittance of the 0.1 % nanofibril suspensions (CNF70, 80 and 90).

The thermal behavior of nanofibrillated celluloses were analyzed using TGA in both air and nitrogen atmospheres (Figure 9) using original dissolving pulp as a reference. Between 25 °C and 100 °C the bound water dehydrated, which caused a 2 % decrease in the sample weight in both atmospheres. At air atmosphere (Figure 9A), all samples except CNF70 clearly had a bimodal TGA curve. The dissolving pulp had an onset temperature of 335 °C. The sample CNF90 had the second highest onset temperature of 272 °C, whereas the samples CNF70 and CNF80 both exhibited onset temperatures at around 264 °C. At 50 % weight loss, the decomposition temperature occurred at 340 °C for dissolving pulp and at 320 °C for nanofibrils, which indicated much faster decomposition of an unmodified pulp. The decreasing trends of onset and decomposition temperatures imply that the thermal stability of pulps decreased due to chemical and mechanical modifications, as had been previously reported.[34,38–42] The amounts of char formed at 590 °C for dissolving pulp, CNF70, CNF80 and CNF90 were 1 %, 8 %, 8 % and 4 %, respectively, confirming that the sample CNF90 had a different chemical structure than the two other modified samples. One explanation for the different thermal behavior of CNF90 compared to CNF70 and CNF80 could be the location of carboxyl groups in the cellulose structure. It has been postulated that the main destabilizing factor in the thermal stability of oxidized celluloses is the presence of a carboxyl group especially at the C6 position.[55] Thus, it is possible that although CNF90 had the highest total carboxyl content, it had less amount of carboxyl groups left at C6 position compared to other samples. A reason for this can be the formation of a cross-link[47] from the carboxyl at the C6 position, which improved the thermal stability.[56] The larger size of the nanoparticles in CNF90 may also have affected the thermal stability.[55]

At N_2 atmosphere (Figure 9B) all samples exhibited a monomodal weight loss curve. The onset temperature for dissolving pulp at N_2 atmosphere was almost identical to the onset temperature for dissolving pulp at air atmosphere (336 °C). Again,

sample CNF90 had the second highest onset temperature at 299 °C, while samples CNF70 and CNF80 had onset temperatures at around 284 °C. Both onset temperatures were about 20 °C higher than the corresponding point at air atmosphere. At 50 % weight loss, the decomposition temperature occurred at 355 °C for dissolving pulp, at 325-330 °C for CNF70 and CNF80, and at 335 °C for CNF90. The amounts of char formed at 590 °C for dissolving pulp, CNF70, CNF80 and CNF90 were 10 %, 32 %, 32 % and 27 %, respectively.

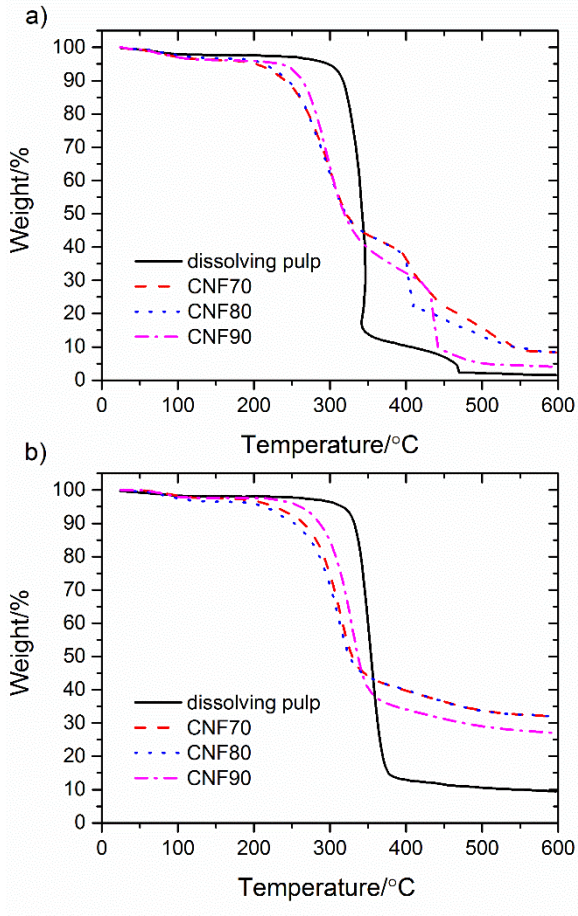

Figure 9. TGA curves of dissolving pulp and cellulose nanofibrils (CNF70, 80 and 90) at a) air and b) nitrogen atmosphere.

The differential thermogravimetric (DTG) curves representing the weight loss rate at different temperatures[57] are presented in Figure 10. According to the results, dissolving pulp had significantly higher weight loss rates than any of the nanofibrils in both atmospheres. At air atmosphere (Figure 10A), the temperature of the maximum weight loss rate of dissolving pulp was at 346 °C. For nanofibrils, the first weight loss rate point occurred at 295 °C. In addition, a second weight loss rate point appeared at 404 °C for CNF70 and CNF80 and at 436 °C for CNF90. However, the decomposition rates of nanofibrils were much slower when compared with the dissolving pulp. At N_2 atmosphere (Figure 10B) the dissolving pulp had the maximum weight loss rate at 352 °C, which is consistent with previous studies.[58] In contrast to the weight loss results obtained at air atmosphere, the nanofibrils did not have the highest weight loss at the same temperature. CNF70 and CNF80 had the maximum weight loss rate at 310 °C, whereas for CNF90 it was at 329 °C. The weight loss rate was slightly higher for CNF90 than for CNF70 and CNF80. The DTG results support the previous findings that CNF90 had a slightly different chemical structure than CNF70 and CNF80, which behaved almost identically to each other in the majority of the analyses.

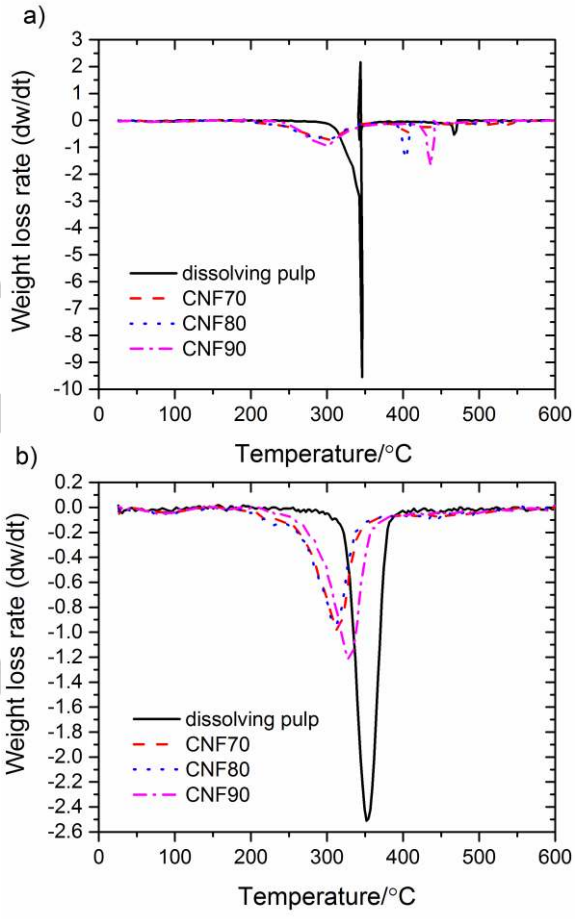

Figure 10. DTG curves of dissolving pulp and cellulose nanofibrils (CNF70, 80 and 90) at a) air and b) nitrogen atmosphere.

Reasoning

Heterogeneous succinylation in urea-LiCl DES was found to efficiently promote the nanofibrillation of softwood dissolving pulp. The main factors influencing the nanofibrillation efficiency were the reaction temperature and the degree of functionalization. The increase in the reaction temperature led to a higher degree of functionalization, but it also decreased the nanofibrillation efficiency. One possible explanation for the outcome is that the

higher temperatures also promoted the side reactions, such as cross-linking, which led to a weaker disintegration of the fibers and higher thermal stability of the nanofibrils when compared to other samples. This implies that depending on the desired end use of the material, the reaction conditions could be tuned to produce either good quality nanofibrillated cellulose or less nanofibrillated but thermally more stable material.

The mechanism on how urea-LiCl DES interacts with the cellulose is currently unknown. Urea-LiCl DES can be categorized as type IV DES, following the example of urea-$ZnCl_2$ DES.[15,59] To our best knowledge, urea-LiCl DES (without water) has not been reported before, and this is also the first time that the functionalization of wood fibers in urea-LiCl DES has been reported. Our group recently demonstrated the usefulness of choline chloride-urea DES pre-treatment in the nanofibrillation of wood cellulose.[32]

It is known that aqueous urea-LiCl mixtures swell regenerated cellulose fibers by penetrating into the cellulose structure and breaking the intermolecular and intramolecular hydrogen bonds.[60–62] However, urea-LiCl-water mixtures do not dissolve cellulose, which would result in destruction of the original cellulose crystalline structure. In addition to the urea-salt mixtures, concentrated salt solutions, or so called molten salt hydrates, from LiCl can swell cellulose fibers,[63,64] and urea containing microemulsions have also been reported to disrupt hydrogen bonding, which promotes cellulose nanofibril production.[65] Moreover, the addition of lithium salts (e.g. LiCl, LiBr) has been proven to increase the dissolution of cellulose in 1-butyl-3-methylimidazolium-based ionic liquid system.[66] It was proposed that the Li^+ ion, once penetrated into the fiber, enhances the cellulose solubility by interacting with the hydroxyl oxygen at the carbon atom 3, which disrupts the hydrogen bond formation between the oxygen atom (O3) and a hydroxyl group's hydrogen atom (H6) at the carbon atom 6 in another cellulose molecule.[66] The lack of water molecules in the lithium salt compared with hydrates ($LiX{\bullet}nH_2O$) leads to more free coordination sites at the lithium cation, enabling stronger interaction between the cellulose hydroxyl groups, which results in efficient breaking of intermolecular and intramolecular hydrogen bonds.

The positive outcome of the swelling is that more reactive sites in cellulose structure are available for reaction with succinic anhydride, which leads to a higher degree of functionalization. In a previous study the swelling was conducted using NaOH treatment (mercerization) prior succinylation, and the treatment was shown to enhance the reaction.[35] The nucleophilic substitution at carbonyl carbon is typically acid catalyzed or base catalyzed, but in our study no catalyst was added to the reaction mixture. Nevertheless, it is possible that ammonia, which was detected in the elemental analysis, has catalyzed the chemical reactions as observed by the increase in the amount of carboxyl groups in the temperature range of 70-90 °C. One explanation for the existence of ammonia in the reaction mixture is the decomposition of urea, which can occur in DES systems already at temperatures below 100 °C.[50]

Conclusions

For the first time, the succinylation of softwood dissolving pulp in urea-LiCl DES and its impact on the nanofibrillation efficiency was investigated. Urea-LiCl DES proved to be a non-degrading and non-dissolving reaction media supported by the DP, which had only a minor drop after the reaction, and the CrI, which decreased only slightly. As the reaction temperature was raised the functionalization was more efficient, but at the same time the probability of the occurrence of side reactions (cross-linking and ammonia formation) increased. The optimal pretreatment condition for dissolving pulp was at a reaction time of 2 h and a reaction temperature of 70-80 °C, which resulted in the production of a highly transparent and viscose nanofibril gel only after three passes through the microfluidizer. The nanofibrils formed an entangled network observed with AFM. The variations in the height distribution between the samples reflected the reaction temperatures and extent of nanofibrillation processes. The thermal stability of the succinylated celluloses decreased upon chemical modification, but the side reactions occurring at higher temperatures improved the thermal stability when compared to the other samples. The usage of a simple and cheap DES-mediated functionalization opens new routes to sustainable cellulose modifications. By further decreasing the reaction time, minimizing the amount of LiCl and studying the possibility to recycle the DES afterwards, the reaction could be made even more environmentally friendly.

Experimental Section

Materials

The cellulose material for the synthesis was prepared by disintegrating dry sheets of commercial softwood dissolving pulp fibers (cellulose 96.2 %, hemicelluloses 3.5 %, total lignin <0.5 %, acetone soluble extractives 0.17 %, Domsjö Fabriker AB, Sweden) in deionized water following a standard procedure, after which the pulp was filtered, washed with technical ethanol, stirred in ethanol for 30 min and filtered again before drying in an oven at 60 °C. Urea (≥97 %, Borealis Biuron®, Austria), LiCl (99 %, Sigma-Aldrich, Germany), succinic anhydride (>95 %, TCI, Japan), ethanol (96 %, VWR, France) and cupriethylenediamine (CED) solution (FF-Chemicals, Finland) were used as received. Deionized water was used throughout the experiments.

Succinylation of cellulose pulp in urea-LiCl DES

The urea-LiCl DES system was prepared by heating and mixing urea (131.45 g) and LiCl (18.55 g) in a beaker at 80 °C in an oil bath for about 30 min or until a clear, colorless liquid was formed. The temperature was set to the desired reaction temperature (70, 80, 90, 100 or 110 °C), and dissolving pulp (1.50 g) and succinic anhydride (9.27 g) were added to the DES, which was then mixed for 2, 6 or 24 hours. The beaker was removed from the oil bath, and ethanol (150 ml) was added while mixing. The resulting mixture was filtered and washed with ethanol (100 ml) and deionized water (1500 ml).

Disintegration of succinylated cellulose to nanofibrils

The modified pulp was diluted to a consistency of 1% in deionized water, after which the pH was adjusted to 8 by adding dilute NaOH solution and was further diluted to a 0.5 % consistency. Then, Ultra Turrax treatment (10 000 rpm) was applied for 1 min. A microfluidizer (Microfluidics M-110EH-30, USA) was used to nanofibrillate the modified pulp. Samples known as SC70 and SC80 (value referring to reaction temperature) were passed three times through 400 µm and 200 µm chambers at a pressure of 1300 bar, while sample SC90 was passed three times through 400 µm and 200 µm chambers at a pressure of 1300 bar, two times through 400 µm and 100 µm chambers at a pressure of 2000 bar and finally once through 200 µm and 87 µm chambers at a pressure of 2000 bar.

Determination of acidic groups

The carboxyl content of the ethanol washed raw pulp and succinylated celluloses before nanofibrillation was analyzed by conductometric titration using a protocol described by Rattaz et al. and Katz et al.[67,68]

Diffuse reflectance infrared Fourier transform

DRIFT spectra of the ethanol washed raw pulp and succinylated celluloses before nanofibrillation was recorded using a Bruker Vertex 80V spectrometer (USA) for oven dried samples. Spectra were taken in the 600-4000 cm^{-1} range, taking 40 scans at a resolution of 2 cm^{-1} for each sample.

Elemental analysis

Elemental analysis of the ethanol washed raw pulp and the succinylated celluloses before nanofibrillation was done in helium atmosphere using a Perkin Elmer CHNS/O 2400 Series II elemental analyzer (USA). Samples were analyzed both before and after acid wash treatment. Samples (0.1 g) were stirred for 30 min in 0.1 M HCl solution (20 ml), after which they were filtered and washed with 0.1 M HCl (50 ml) and deionized water (500 ml). Before analysis, the pulps were dried in an oven (60 °C).

Degree of polymerization

The average DP of ethanol washed raw pulp and succinylated celluloses before nanofibrillation was evaluated from the limiting viscosity, measured in cupriethylenediamine-solution according to the ISO 5351 standard. Samples were oven dried (60 °C) prior to the measurements. The limiting viscosity values were converted to DP using equation (1)

DP = ((1.65[η] - 116H)/ C) ^1.111 (1)

where [η] is the limiting viscosity, C is the mass fraction of cellulose and H is the mass fraction of hemicellulose. This calculation makes a correction for the contribution of hemicellulose to the limiting viscosity number and DP of cellulose, assuming that the average DP of hemicellulose is 140. As there exist different standards and equations to calculate DP of cellulose, DP values were mainly used to compare the effect of the DES treatment on the cellulose pulp.

X-ray diffraction

The crystallinity of the ethanol washed raw pulp, succinylated celluloses and nanofibrillated samples were analyzed using wide-angle X-ray diffraction (WAXD). Measurements were conducted on a Rigaku SmartLab 9 kW rotating anode diffractometer (Japan) using a Co Kα radiation (40 kV, 135 mA) (λ = 1.79030 nm). Tablets with a thickness of 1 mm were pressed from freeze-dried cellulose samples. Scans were taken over a 2θ (Bragg angle) range from 5° to 50° at a scanning speed of 10°/s, using a step of 0.05° or 0.1°. The degree of crystallinity in terms of the crystallinity index (CrI) was calculated from the peak intensity of the main crystalline plane (200) diffraction (I_{200}) at 26° and from the peak intensity at 21.6° associated with the amorphous fraction of cellulose (I_{am}) according to equation (2).

$$CrI = ((I_{200} - I_{am})/ I_{200}) \times 100\ \%\ (2)$$

It should be noted that due to Co Kα radiation source, the cellulose peaks have different diffraction angles than the results obtained by Cu Kα radiation source.

Atomic force microscopy

Atomic force microscopy (MultiMode8, Bruker, Germany) was used for topography imaging of cellulose nanofibrils. The aqueous 0.001 % nanofibril suspension was sonicated for 1 min prior usage. The samples were prepared by drop casting the suspension (20 µl) onto a freshly cleaved mica surface (Highest Grade V1 Mica Discs 12 mm, Ted Pella Inc., USA). After 5 min, the excess amount of the suspension was removed from the mica by touching the droplet with a corner of a filter paper, and the surface was allowed to dry for few minutes. AFM was operated using ScanAsyst™ in air. Triangular Si probes with a tip radius of 2 nm and nominal spring constant of 0.4 Nm^{-1} (Scanasyst-Air, Bruker, USA) were used for imaging acquisition. For each sample, topography images with scan size of 5 × 5 μm^2 were acquired in 10 different surface locations. Imaging processing and analysis was performed using the Gwyddion 2.44 software (Department of Nanometrology, Czech Metrology Institute). The height distribution was obtained by measuring the height profile of 100 nanofibrils for each sample. The height distribution peak and width obtained for each sample was evaluated via Gaussian fitting using the OriginPro software (OriginLab Corporation, USA).

Optical transmittance

The transmittance of 0.1 % nanofibril suspensions was measured at wavelengths of 350-800 nm with a Shimadzu UV–Vis spectrometer (Japan) using glass cuvettes. Two scans were taken at a resolution of 1 nm for each sample. Deionized water was used as a reference.

Viscosity

The low shear viscosities of 0.2 % nanofibril suspensions were recorded at a temperature of 20 °C at 10, 20, 50 and 100 RPM using a Brookfield DV-II+ Pro EXTRA viscometer (USA) using a vane-shaped spindle (V-73).

Thermogravimetric analysis

TGA measurements were carried out with a thermal analyzer Netzsch STA 409 PC/PG apparatus (Germany) in two different atmospheres—under nitrogen flow and under air flow (dynamic air)—both with a constant rate of 60 ml min^{-1}. Each measurement was made using ca. 5 mg of the freeze-dried nanofibrillated sample placed in Pt crucible, which was heated from 25 °C to 600 °C at a scanning rate of 10 °C min^{-1}. The temperature of polymer degradation, Td, was taken as a temperature at the onset point of the weight loss in the TGA curve obtained.

Acknowledgements

The financial support of the Advanced Materials Doctoral Program (ADMA-DP) of the University of Oulu Graduate School is greatly acknowledged. Ms. Katariina Kauppila is acknowledged for her kind assistance in laboratory experiments, and Mrs. Elisa Wirkkala is acknowledged for performing the elemental analysis and limiting viscosity measurements. We would like to also thank Mr. Sami Saukko from the Center of Microscopy and Nanotechnology for the XRD measurements, and Mr. Tommi Kokkonen from the Centre for Advanced Steels Research of the University of Oulu for the TGA measurements.

Keywords: biomass • cellulose • deep eutectic solvent • green chemistry • nanocellulose

[1] D. A. Alonso, A. Baeza, R. Chinchilla, G. Guillena, I. M. Pastor, D. J. Ramón, *Eur. J. Org. Chem.* **2016**, *2016*, 612–632.
[2] R. A. Sheldon, *Chem. Soc. Rev.* **2012**, *41*, 1437–1451.
[3] F. del Monte, D. Carriazo, M. C. Serrano, M. C. Gutiérrez, M. L. Ferrer, *ChemSusChem* **2014**, *7*, 999–1009.
[4] S. Khaksar, *J. Fluor. Chem.* **2015**, *172*, 51–61.
[5] X. Zhang, S. Heinonen, E. Levänen, *RSC Adv* **2014**, *4*, 61137–61152.
[6] Y. Gu, F. Jérôme, *Green Chem.* **2010**, *12*, 1127–1138.
[7] E. García-Verdugo, B. Altava, M. I. Burguete, P. Lozano, S. V. Luis, *Green Chem.* **2015**, *17*, 2693–2713.
[8] S. R. Labafzadeh, K. J. Helminen, I. Kilpeläinen, A. W. T. King, *ChemSusChem* **2015**, *8*, 77–81.
[9] A. M. Da Costa Lopez, R. Bogel-Lukasik, *ChemSusChem* **2015**, *8*, 947–965.
[10] C. C. Teo, S. N. Tan, J. W. H. Yong, C. S. Hew, E. S. Ong, *J. Chromatogr. A* **2010**, *1217*, 2484–2494.
[11] M. Cvjetko Bubalo, S. Vidović, I. Radojčić Redovniković, S. Jokić, *J. Chem. Technol. Biotechnol.* **2015**, *90*, 1631–1639.
[12] A. P. Abbott, G. Capper, D. L. Davies, R. K. Rasheed, V. Tambyrajah, *Chem. Commun.* **2003**, 70–71.
[13] A. P. Abbott, D. Boothby, G. Capper, D. L. Davies, R. K. Rasheed, *J. Am. Chem. Soc.* **2004**, *126*, 9142–9147.
[14] A. P. Abbott, T. J. Bell, S. Handa, B. Stoddart, *Green Chem.* **2006**, *8*, 784–786.
[15] A. P. Abbott, J. C. Barron, K. S. Ryder, D. Wilson, *Chem. - Eur. J.* **2007**, *13*, 6495–6501.
[16] Q. Zhang, K. De Oliveira Vigier, S. Royer, F. Jérôme, *Chem. Soc. Rev.* **2012**, *41*, 7108–7146.
[17] D. V. Wagle, H. Zhao, G. A. Baker, *Acc. Chem. Res.* **2014**, *47*, 2299–2308.
[18] K. Radošević, M. Cvjetko Bubalo, V. G. Srček, D. Grgas, T. L. Dragičević, I. R. Redovniković, *Ecotoxicol. Environ. Saf.* **2015**, *112*, 46–53.
[19] B.-Y. Zhao, P. Xu, F.-X. Yang, H. Wu, M.-H. Zong, W.-Y. Lou, *ACS Sustain. Chem. Eng.* **2015**, *3*, 2746–2755.
[20] M. Hayyan, M. A. Hashim, A. Hayyan, M. A. Al-Saadi, I. M. AlNashef, M. E. S. Mirghani, O. K. Saheed, *Chemosphere* **2013**, *90*, 2193–2195.
[21] K. Radošević, J. Železnjak, M. Cvjetko Bubalo, I. R. Redovniković, I. Slivac, V. G. Srček, *Ecotoxicol. Environ. Saf.* **2016**, *131*, 30–36.
[22] P. T. Anastas, J. C. Warner, *Green Chemistry: Theory and Practice*, Oxford University Press, Oxford, **1998**, pp. 29-55.
[23] J. A. Sirviö, H. Liimatainen, J. Niinimäki, O. Hormi, *RSC Adv.* **2013**, *3*, 16590–16596.
[24] T. Suopajärvi, H. Liimatainen, O. Hormi, J. Niinimäki, *Chem. Eng. J.* **2013**, *231*, 59–67.
[25] T. Suopajärvi, E. Koivuranta, H. Liimatainen, J. Niinimäki, *J. Environ. Chem. Eng.* **2014**, *2*, 2005–2012.
[26] T. Suopajärvi, H. Liimatainen, M. Karjalainen, H. Upola, J. Niinimäki, *J. Water Process Eng.* **2015**, *5*, 136–142.
[27] O. Nechyporchuk, M. N. Belgacem, J. Bras, *Ind. Crops Prod.* **2016**, DOI 10.1016/j.indcrop.2016.02.016.
[28] H. Liimatainen, M. Visanko, J. A. Sirviö, O. E. O. Hormi, J. Niinimaki, *Biomacromolecules* **2012**, *13*, 1592–1597.
[29] H. Liimatainen, M. Visanko, J. Sirviö, O. Hormi, J. Niinimäki, *Cellulose* **2013**, *20*, 741–749.
[30] H. Liimatainen, T. Suopajärvi, J. Sirviö, O. Hormi, J. Niinimäki, *Carbohydr. Polym.* **2014**, *103*, 187–192.
[31] M. Hietala, A. Ämmälä, J. Silvennoinen, H. Liimatainen, *Cellulose* **2016**, *23*, 427–437.
[32] J. A. Sirviö, M. Visanko, H. Liimatainen, *Green Chem.* **2015**, *17*, 3401–3406.
[33] F. Gellerstedt, P. Gatenholm, *Cellulose* **1999**, *6*, 103–121.
[34] C. F. Liu, R. C. Sun, M. H. Qin, A. P. Zhang, J. L. Ren, J. Ye, W. Luo, Z. N. Cao, *Bioresour. Technol.* **2008**, *99*, 1465–1473.
[35] L. V. A. Gurgel, O. K. Júnior, R. P. de F. Gil, L. F. Gil, *Bioresour. Technol.* **2008**, *99*, 3077–3083.
[36] X. Yin, C. Yu, X. Zhang, J. Yang, Q. Lin, J. Wang, Q. Zhu, *Polym. Bull.* **2011**, *67*, 401–412.
[37] C. F. Liu, R. C. Sun, A. P. Zhang, J. L. Ren, Z. C. Geng, *Polym. Degrad. Stab.* **2006**, *91*, 3040–3047.
[38] C. F. Liu, R. C. Sun, A. P. Zhang, J. L. Ren, X. A. Wang, M. H. Qin, Z. N. Chao, W. Luo, *Carbohydr. Res.* **2007**, *342*, 919–926.
[39] W. Y. Li, A. X. Jin, C. F. Liu, R. C. Sun, A. P. Zhang, J. F. Kennedy, *Carbohydr. Polym.* **2009**, *78*, 389–395.
[40] C. F. Liu, A. P. Zhang, W. Y. Li, F. X. Yue, R. C. Sun, *Ind. Crops Prod.* **2010**, *31*, 363–369.
[41] M. E. Gibril, L. Huan, L. haiFeng, L. X. Da, Z. Yue, K. Han, Y. Muhuo, *RSC Adv.* **2013**, *3*, 1021–1024.
[42] W. Shang, Z. Sheng, Y. Shen, B. Ai, L. Zheng, J. Yang, Z. Xu, *Carbohydr. Polym.* **2016**, *141*, 135–142.
[43] W. Zhang, C. Li, M. Liang, Y. Geng, C. Lu, *J. Hazard. Mater.* **2010**, *181*, 468–473.
[44] P. Huang, M. Wu, S. Kuga, D. Wang, D. Wu, Y. Huang, *ChemSusChem* **2012**, *5*, 2319–2322.
[45] S. Hokkanen, E. Repo, M. Sillanpää, *Chem. Eng. J.* **2013**, *223*, 40–47.
[46] D. Ray, B. K. Sarkar, *J. Appl. Polym. Sci.* **2001**, *80*, 1013–1020.
[47] T. Yoshimura, K. Matsuo, R. Fujioka, *J. Appl. Polym. Sci.* **2006**, *99*, 3251–3256.
[48] S. Y. Oh, D. I. Yoo, Y. Shin, G. Seo, *Carbohydr. Res.* **2005**, *340*, 417–428.
[49] X. Gu, C. Q. Yang, *Res. Chem. Intermed.* **1998**, *24*, 979–996.
[50] S. P. Simeonov, C. A. M. Afonso, *RSC Adv.* **2016**, *6*, 5485–5490.
[51] L. T. T. Vo, B. Široká, A. P. Manian, T. Bechtold, *Carbohydr. Polym.* **2010**, *82*, 1191–1197.
[52] C. Yin, X. Shen, *Eur. Polym. J.* **2007**, *43*, 2111–2116.
[53] I. Besbes, S. Alila, S. Boufi, *Carbohydr. Polym.* **2011**, *84*, 975–983.
[54] I. Besbes, M. R. Vilar, S. Boufi, *Carbohydr. Polym.* **2011**, *86*, 1198–1206.
[55] P. R. Sharma, A. J. Varma, *Carbohydr. Polym.* **2014**, *114*, 339–343.
[56] Y. Niu, X. Zhang, X. He, J. Zhao, W. Zhang, C. Lu, *Int. J. Biol. Macromol.* **2015**, *72*, 855–861.
[57] J. A. Sirviö, T. Hasa, J. Ahola, H. Liimatainen, J. Niinimäki, O. Hormi, *Carbohydr. Polym.* **2015**, *133*, 524–532.
[58] R. P. Swatloski, S. K. Spear, J. D. Holbrey, R. D. Rogers, *J. Am. Chem. Soc.* **2002**, *124*, 4974–4975.
[59] H. Lian, S. Hong, A. Carranza, J. D. Mota-Morales, J. A. Pojman, *RSC Adv.* **2015**, *5*, 28778–28785.
[60] I. Tatárová, A. P. Manian, B. Široká, T. Bechtold, *Cellulose* **2010**, *17*, 913–922.
[61] I. Tatárová, W. MacNaughtan, A. P. Manian, B. Široká, T. Bechtold, *Macromol. Mater. Eng.* **2012**, *297*, 540–549.
[62] T. Bechtold, A. P. Manian, H. B. Öztürk, U. Paul, B. Široká, J. Široký, H. Soliman, L. T. T. Vo, H. Vu-Manh, *Carbohydr. Polym.* **2013**, *93*, 316–323.
[63] H. Leipner, S. Fischer, E. Brendler, W. Voigt, *Macromol. Chem. Phys.* **2000**, *201*, 2041–2049.
[64] E. Brendler, S. Fischer, H. Leipner, *Cellulose* **2001**, *8*, 283–288.
[65] C. A. Carrillo, J. Laine, O. J. Rojas, *ACS Appl. Mater. Interfaces* **2014**, *6*, 22622–22627.
[66] A. Xu, J. Wang, H. Wang, *Green Chem.* **2010**, *12*, 268–275.
[67] A. Rattaz, S. P. Mishra, B. Chabot, C. Daneault, *Cellulose* **2011**, *18*, 585–593.
[68] S. Katz, R. P. Beatson, A. M. Scallan, *Sven. Papperstidning* **1984**, *87*, R48-53.

Entry for the Table of Contents

Layout 2:

FULL PAPER

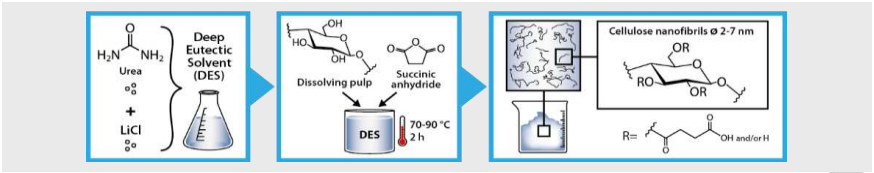

*Tuula Selkälä, Juho Antti Sirviö, Gabriela S. Lorite and Henrikki Liimatainen**

Page No. – Page No.

Anionically Stabilized Cellulose Nanofibrils via Succinylation Pre-Treatment in Urea-LiCl Deep Eutectic Solvent

Urea-LiCl deep eutectic solvent was successfully used as an alternative reaction media in the succinylation of dissolving cellulose pulp. Consequent mechanical disintegration of the functionalized fibers resulted in the formation of a highly viscose and transparent gel comprising of a network of anionic cellulose nanofibrils with a diameter of 2-7 nm.